Proceedings of ERAD 2006

# Impact of different tracing methodologies in a nowcasting technique

**Virginia Poli[1,2], Mario Montopoli[2,3], Pier Paolo Alberoni[1,4], Frank S. Marzano[3,5]**

[1] ARPA - SIM, Bologna (Italy).

[2] CIMA - Università di Genova e della Basilicata, Savona (Italy).

[3] Dipartimento di Ingegneria Elettrica – Centro di Eccellenza CETEMPS - Università dell'Aquila, L'Aquila (Italy).

[4] ISAC - CNR, Bologna (Italy).

[5] Dipartimento di Ingegneria Elettronica – Università "La Sapienza" di Roma, Roma (Italy).

## 1 Introduction

The nowcasting technique used in this work exploits an algorithm that analyzes reflectivity/precipitation radar patterns and extrapolates coherent structures ahead in the future using a semi-lagrangian scheme feed by steering vector fields.

A particular effort is gathered to define motion fields and to analyze the relative differences; to meet this goal two techniques are used to identify the tracers within the radar map.

The first is based on a multi-scale recursive cross-correlation analysis of reflectivity pattern. This operation involves areas bounded by values subjectively chosen and leads up to the definition of a three-level motion vectors. The areas are defined as a geometrical segmentation of the radar map as a function of reflectivity level analyzed.

The second method is introduced in order to identify objects over the radar image. Cross-correlation between successive images is carried out between areas covering convective raincells identified using an adaptive scheme based on the spatial correlation of the local rainfall field.

In both cases retrieved vectors are merged to provide a motion field for the entire radar coverage to be used within the same semi-lagrangian advection scheme.

The comparison of the two methods will be discussed on representative cases.

*Correspondence to:* Virginia Poli.

vpoli@arpa.emr.it

## 2 Definition of steering vector fields

### 2.1 Background motion field

For background motion field is intended the average motion of the whole reflectivity pattern. It is estimated starting from radar patterns identified by a very low reflectivity value (0 dBZ) applying a cross-correlation analysis.

For two subsequent data fields, an area centered on radar image is considered. The one from field at time $t_0$ is shifted around the one at time $t_1=t_0+15$ minutes in order to determine in what position and in what direction cross-correlation coefficient is maximum. Translations between selected areas are performed with an angular step of 30° and with a radial step of 1 Km (with an upper limit of 20 Km).

Best cross-correlation coefficient determines components of

steering vector for this layer. To reduce the variability of this vector in time and to avoid abrupt spatial variations in reflectivity field, a weighted average in time of motion vector estimated is made (Poli et al., 2006).

### 2.2 Tracer 1: reflectivity levels

Keeping in mind that movement of precipitation structures is a function of scale, a multi-scale recursive cross-correlation analysis is applied to two layers bounded by reflectivity values higher than the one that characterizes background. In particular they are equal to 30 and 50 dBZ.

In this case cross-correlation is implemented on radar scans divided in regular grids. They have a resolution depending on reflectivity value considered. Each box of the grid of the first scan is compared to all possible box in a range of 20 Km in the second scan until maximum cross-correlation coefficient is derived. Also in this case values calculated are used to retrieve components of motion vectors.

Final motion field ensues from the weighted sum of motion vectors of each level (Figures 1 and 2). Weight is an exponential function of the relative displacement between vectors and analysis gridpoint and depends on the reflectivity level considered. In particular higher reflectivity are supposed to be representative of smaller structures and hence smaller influence area (Poli et al., 2005).

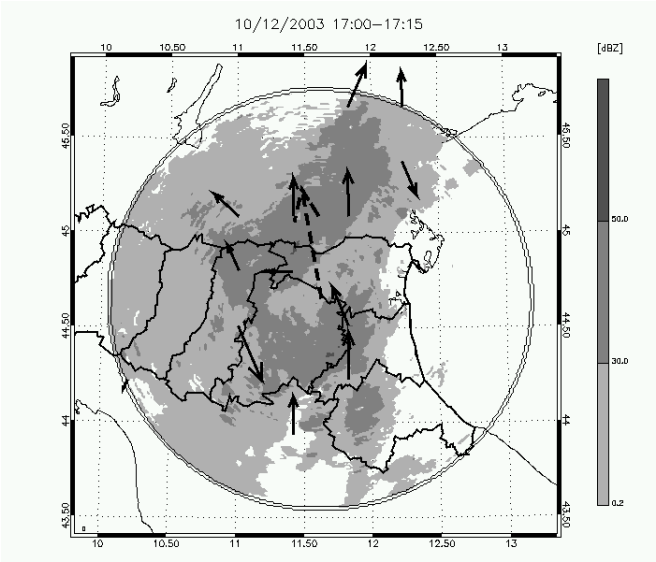


**Fig. 1.** Motion vectors retrieved for each reflectivity layer: background (dashed) and 30 dBZ reflectivity level (continuous). In this case no vector is identified for the second reflectivity layer (50 dBZ).

### 2.3 Tracer 2: convective raincells

In the second method some areas are selected on reflectivity radar maps in order to be used in cross-correlation analysis. Informations on dimension and position of these areas come from an adaptive and accurate algorithm for raincell identification which provides a spatial characterization of mid-latitude mesoscale rain fields from C-band radar measurements. The procedure adopts variable and adapting thresholds based on spatial autocorrelation of local rainfall field and delineate single raincells (Figure 3) which are, potentially, convective cores (Montopoli et al., 2006).

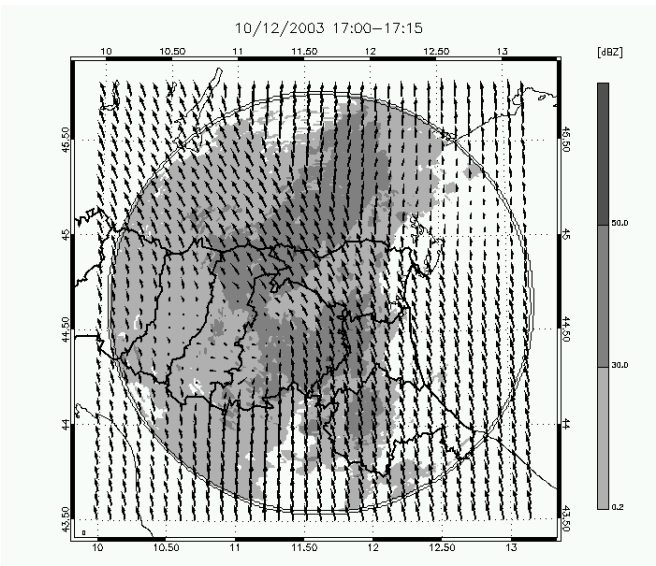


**Fig. 2.** Motion field generated starting from vectors of Figure 1.

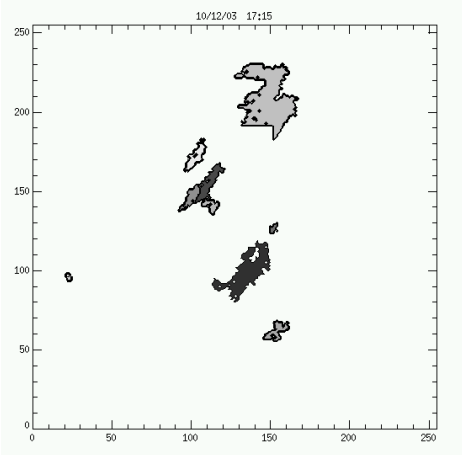


**Fig. 3.** Raincells individuated at 17:15 on 10 December 2003.

The outcome of the cross-correlation step is a number of vector as much as are objects investigated. Subsequently single vectors and background motion field (Figure 4) are merged in the definitive steering field (Figure 5). In this procedure extent of each object is considered in a way that larger areas weighs much more than small ones.

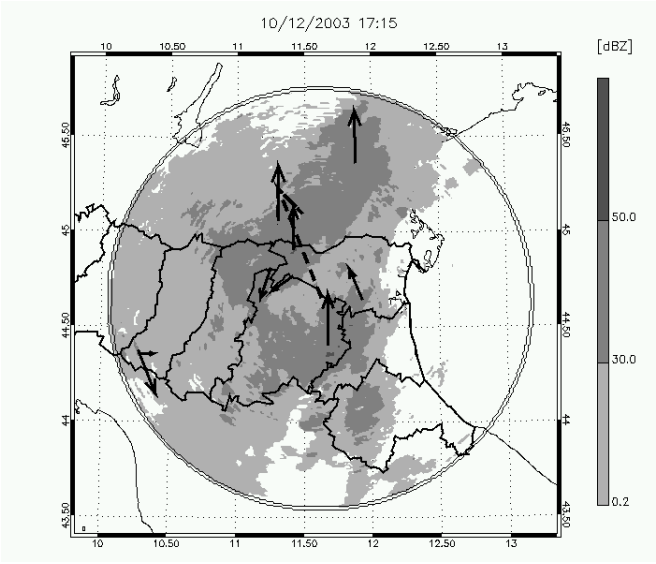


**Fig. 4.** Vectors retrieved using raincell as tracer superimposed at background motion field (dashed). Instant analyzed is the same of figure 1.

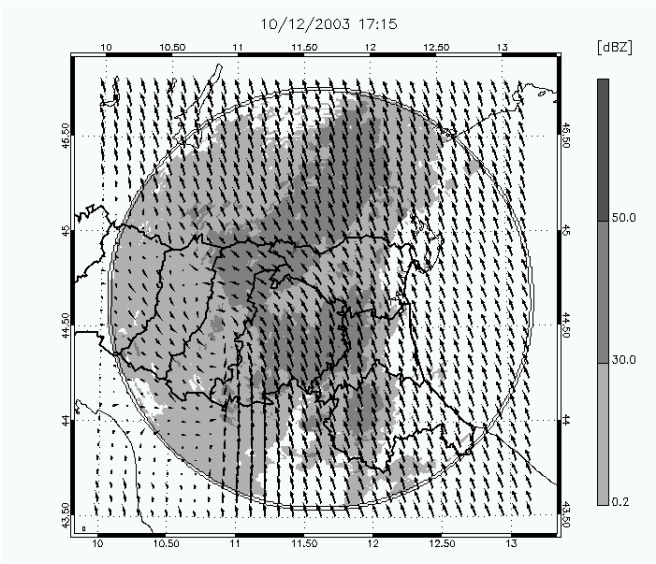


**Fig. 5.** Steering motion field obtained using vectors of Figure 4.

## 3 Case study

The comparison of the two methods is carried out from the study of an episode in Po valley in December 2003. The event is characterized by a low reflectivity due to persistent precipitations during almost the whole day. Data come from S.Pietro Capofiume radar. Resolution of images is 15 minutes in time and 1km in space.

In order to evaluate forecast performances due to different motion fields used, common indexes such as critical success index (CSI), false alarm rate (FAR), probability of detection (POD), true skill statistic (TSS) and equitable threat score (ETS) are calculated even if this type of verification is insensitive to the size of location and timing errors and it is highly sensitive to scaling of observations and forecasts (Brown et al., 2002). This analysis concerns only pixels with reflectivity greater than 30 dBZ.

In Tables 1 and 2 values of estimated averaging results on the whole event are stored. Figures 6, 7 and 8 show the trend of some parameters for a selected forecast.

**Table 1.** Scores mean values calculated using reflectivity levels as tracer.

| Tracer: reflectivity levels | | | | | |
|---|---|---|---|---|---|
| Lead time | CSI | POD | FAR | ETS | TSS |
| +15 min | 0.4775 | 0.6416 | 0.3574 | 0.4302 | 0.5987 |
| +30 min | 0.3444 | 0.5092 | 0.4969 | 0.2918 | 0.4508 |
| +45 min | 0.2651 | 0.4166 | 0.5915 | 0.2112 | 0.3482 |
| +60 min | 0.2100 | 0.3489 | 0.6613 | 0.1569 | 0.2740 |
| +90 min | 0.1488 | 0.2631 | 0.7469 | 0.0993 | 0.1822 |
| +120 min | 0.1138 | 0.2118 | 0.7949 | 0.0685 | 0.1313 |

**Table 2.** Same as for Table 1, with raincells in place of reflectivity layers.

| Tracer: convective rain cells | | | | | |
|---|---|---|---|---|---|
| Lead time | CSI | POD | FAR | ETS | TSS |
| +15 min | 0.4571 | 0.6216 | 0.3725 | 0.4084 | 0.5766 |
| +30 min | 0.3313 | 0.4959 | 0.5013 | 0.2787 | 0.4373 |
| +45 min | 0.2565 | 0.4059 | 0.5897 | 0.2035 | 0.3391 |
| +60 min | 0.2058 | 0.3517 | 0.6537 | 0.1544 | 0.2806 |
| +90 min | 0.1329 | 0.2369 | 0.7546 | 0.0866 | 0.1625 |
| +120 min | 0.0977 | 0.1837 | 0.8014 | 0.0576 | 0.1132 |

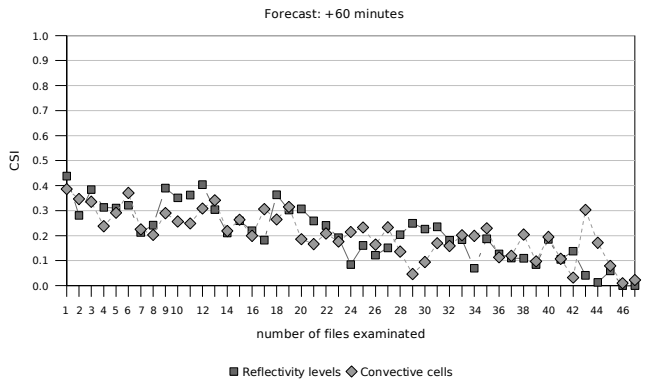


**Fig. 6.** Trend of CSI during the entire event for the forecast with 1 hour lead time. Outcomes of the use of different tracer are compared.

## 4 Conclusions

The issue of this work is to understand the influence of two different tracers in the definition of different motion fields which are used as input for a semi-lagrangian advection

algorithm.

Substantially there is no improvement in changing the tracer, even if motion fields retrieved can be very different. One of the causes that limits second method used can be its strong dependence on the number and dimension of raincells. There is no control on spatial continuity of vectors direction. This means that one cell direction can be the exact opposite of neighbouring.

Selecting a stratiform event could not be the right choice to test the method. Nature of the event (especially the type of precipitation and the degree of spatial organization of the rainfall field) has an important effect on the quality of forecasts.

Verification indexes prove the sparse reliability of forecast with lead times greater than 1 hour. As stressed by Mecklenburg et al. (2000), lead times for useful forecasts are less than 2 hours and often less than 1 hour. FAR measures the fraction of event forecasts which were actually non-events. It increases rapidly reaching almost its maximum value, while the other indexes become negligible (Figure 9).

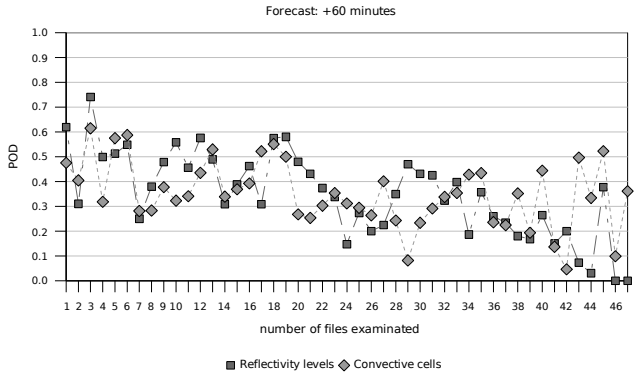


**Fig. 7.** Same as for Figure 6, but for POD index.

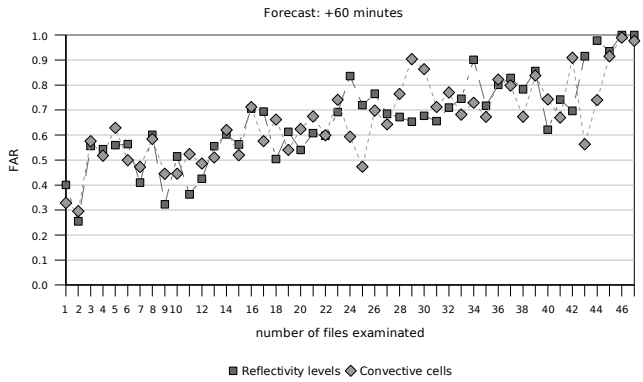


**Fig. 8.** Same as for Figure 6, but for FAR index.

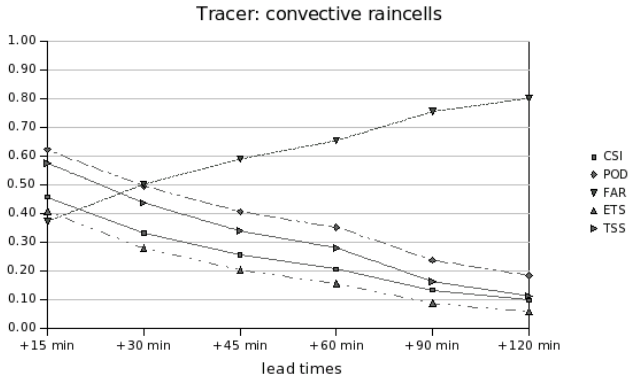


**Fig. 9.** Tendency of estimated indexes for increasing lead times.

*Acknowledgements:* This activity is carried on in the framework of PROSCENIO and is partially supported by the European Union under the INTERREG IIIB CADSES programme "RISK-AWARE", contract number 3B064.

## References

Brown, B. G., J. L. Mahoney, C. A. Davis, R. Bullock and C. K. Mueller, 2002: Improved approaches for measuring the quality of convective weather forecasts. 16th Conference on Probability and Statistic in Atmospheric Sciences, Orlando, FL, *Amer. Meteor. Soc.*, 20-25.

Mecklenburg, S., J. Joss,W. Schmid, 2000: Improving the nowcasting of precipitation in an Alpine region with an enhanced radar echo tracking algorithm. *J. Hydrol.*, **239**, 46-68.

Montopoli, M., F.S. Marzano, G. Vulpiani, A. Fornasiero, P. P. Alberoni, L. Ferraris and N. Rebora, 2006: Spatial characterization of raincell horizontal profiles from C-band radar measurements at mid-latitude. *Ad. Geo.*, Submitted.

Poli V., P. P. Alberoni, T. Paccagnella and D. Cesari, 2005: Preliminary results of the comparison of two advection methods. *WWRP Symposium no Nowcasting and Very Short Range Forecasting*, Toulouse, France, 5-9 September 2005.

Poli, V., P. P. Alberoni and D. Cesari, 2006: Preliminary analysis of the intercomparison of two nowcasting methods. *MAP*, Risk-AWARE special issue, Submitted.